Journal of Advances in Mathematics and Computer Science

27(4): 1-22, 2018; Article no.JAMCS.41767
ISSN: 2456-9968
(Past name: British Journal of Mathematics & Computer Science, Past ISSN: 2231-0851)

A Bioconvection Model for Squeezing Flow between Parallel Plates Containing Gyrotactic Microorganisms with Impact of Thermal Radiation and Heat Generation/Absorption

Syed Asif Hussain[1,2], Sher Muhammad[1,2*], Gohar Ali[1], Syed Inayat Ali Shah[1], Mohammad Ishaq[1], Zahir Shah[3], Hameed Khan[4], Mohammad Tahir[1] and Muhammad Naeem[2]

[1]Department of Mathematics, Islamia College Peshawar, 25000, KP, Pakistan.
[2]CECOS University of IT & Emerging Science Peshawar, 25000, KP, Pakistan.
[3]Department of Mathematics, Abdul Wali Khan University, Mardan, KP, Pakistan.
[4]Department of Physics, Hazara University Mansehra, Hazara, 21300, KP, Pakistan.

Authors' contributions

This work was carried out in equal collaboration of all the authors. The final version of the manuscript has been read and approved by the authors.

Article Information

DOI: 10.9734/JAMCS/2018/41767
Editor(s):
(1) Mohammad Reza Safaei, Professor, Faculty of Electrical and Electronics Engineering, Division of Computational Physics, Institute for Computational Science, Ton Duc Thang University, Ho Chi Minh City, Vietnam.
Reviewers:
(1) G. Sarojamma, Sri Padmavati Mahila Visvavidyalayam, India.
(2) Muhammad Mubashir Bhatti, Shanghai University, China.
Complete Peer review History: http://www.sciencedomain.org/review-history/24973

Original Research Article

Received: 24th March 2018
Accepted: 30th May 2018
Published: 5th June 2018

Abstract

The aim of present paper is to investigate the bioconvection squeezing nanofluid flow between two parallel plates' channels. One of the plates is stretched and the other is fixed. In this study water is considered as a base fluid because microorganisms can survive only in water. The significant influences of thermophoresis and Brownian motion have also been taken in nanofluid model. A highly nonlinear and coupled system of partial differential equations presenting the model of bioconvection flow between parallel plates is reduced to a nonlinear and coupled system (non-dimensional bioconvection flow model) of ordinary differential equations with the help of feasible non-dimensional variables. The acquired nonlinear system has been solved via homotopy analysis method (HAM). The convergence of the method has been shown numerically. Also, influence of various parameters has been discussed for the non-dimensional velocity, temperature, concentration and density of the motile microorganisms both for suction and injection cases. The variation of the Skin friction, Nusselt number, Sherwood number and

**Corresponding author: E-mail: shermuhammad@cecos.edu.pk;*

their effects on the velocity, concentration, temperature and the density motile microorganism profiles are examined. Furthermore, for comprehension the physical presentation of the embedded parameters, such as unsteady squeezing parameter, Thermal radiation parameter, Peclet number, Thermophoresis parameter, Levis number, Prandtl number, Schmidt number and Brownian motion are plotted and discussed graphically. At the end, we make some concluding remarks in the light of this article.

Keywords: Thermal radiation; gyrotactic microorganisms; squeezing flow; nanofluid; parallel plates; and HAM.

1 Introduction

Nanofluids have attracted the interest of researchers due to their numerous potential applications in industrial processes, such as in power generation, chemical processes and heating or cooling processes and also in nanotechnology. Bio-convection is a phenomenon that occurs when microorganisms (which are denser than water) swim upward on average. Due to up swimming the microorganisms involved such as gyro tactic microorganisms like algae tend to concentrate in the upper portion of the fluid layer thus causing a top heavy density stratification that often becomes unstable. The study of nanofluid bio-convection describing the spontaneous pattern formation and density stratification induced by the simultaneous interaction of the denser self-propelled microorganisms, nanoparticles and buoyancy forces seems necessary. These microorganisms may include gravitaxis or oxytaxis organisms. The addition of gyrotactic microorganisms into the nanofluid increases its stability as a suspension.

The squeezing nanofluid flow has many applications in different fields, particularly in chemical engineering and food industry. There are many examples regarding squeezing flow, but especially the important ones are compression, injection and polymer preparation. This field got considerable attention due to useful applications in the Biophysical and Physical field. Stefan [1] has been explored squeezing flow using lubrication approximation. Verma [2] has been discussed squeezing flow of nanofluid between parallel plates. Magneto hydrodynamic squeezed flow of nanofluid over a sensor surface is investigated by Haq et al. [3] Features of unsteady squeezing flow of nanofluids between two parallel plates are investigated by Gupta and Ray [4]. Qayyum et al. [5] analyzed the time dependent squeezing flow of Jeffrey fluid between two parallel disks. Hayat et al. [6] analyzed mixed convection squeezing flow of an incompressible Newtonian fluid between two vertical plates. Hayat et al. [7] has been investigated magneto-hydrodynamic (MHD) in squeezing flow in Jeffery nanofluid for the parallel disc. Dib et al. [8] has examined squeezing nanofluids flow analytically. Nano-fluid is the composition of Nano-particles, which shows significant properties at a reticent concentration of Nano-particles. Nano-fluid is a term refers to liquid consisting sub microparticles. It has many applications, but the important feature is the development of thermal conductivity observed by Masuda et al. [9]. His study reveals that Nano-fluid has different thermal properties like thermal viscosity, thermal infeasibility, relocate of temperature, convection temperature and thermal conductivity as compared to oil and water base fluids [10-11].

Muhammad et al. [12] investigated the rotating flow of magneto hydrodynamic carbon nanotubes over a stretching sheet with the impact of non-linear thermal radiation and heat generation/absorption. Hamad [13] has been investigated the Nano-fluid analytical solution for convection flow in the presence of a magnetic field. Kaufi et al. [14] has been studied current of Nano-fluid. Sheikholeslami [15] has been investigated thermal radiation effect on MHD flow and relocate of temperature by two-phase mode. Khan et al. [16] studied the combined magneto hydrodynamic and electric field effect on an unsteady Maxwell nanofluid flow over a stretching surface under the influence of variable heat and thermal radiation.

Goodman [17] was the first one to explored viscous fluid in parallel plates. Sheikholeslami et al. [18-19] has been discussed the nanofluid flow of viscous fluids between parallel plates with rotating systems in three dimensions under the magneto hydrodynamics (MHD) effects. For the solution of the modelled problems they used numerical method and discussed the special effects of achieving parameters in detail. Attia et al.

[20] has been inspected viscous flow between parallel plates with magnetohydrodynamics. Mahmoodi and Kandelousi [21] have studied the hydro magnetic impact of Kerosene−alumina nanofluid flow in the occurrence of heat transfer analysis, differential transformation method is used in their work. Tauseef et al. [22] and Rokni et al. [23] have been examined the MHD and temperature effects on nanofluids flow in parallel plates with the rotating system. Hayat et al. [24] has been discussed thermal radiations effect in squeezing flows of Jeffery nanofluids. Ali et al. [25] has discussed the effect of radiations on un-steady free convection magnetohydrodynamics flows of the Brinkman kind fluids in a porous medium have Newtonian heat. Khan et al. [26] have been observed thermal radiation consequence on squeezing flow Casson fluid among parallel disks. Srinivasacharya [27] has been investigated both the effects in the vertical curly surface at existing of the porous medium.

The idea of Gyrotactic microorganisms develops the stability of nanoparticles in the suspension [28]. Among numerous ways of improving, the stability of nanoparticles and heat transfer in fluid gyrotactic microorganisms study an important one. Bhatti et al. [29] has investigated Simultaneous effects of coagulation and variable magnetic field on peristaltically induced motion of Jeffrey nanofluid containing gyrotactic microorganism. Shahid et al. [30] investigated magneto hydrodynamics nanofluid flow containing gyrotactic microorganisms propagating over a stretching surface by successive Taylor series linearization method.Abbas et al. [31] investigated Electro magneto hydrodynamic nanofluid flow past a porous Riga plate containing gyrotactic microorganism. Bhatti et al. [32] have been investigated A mathematical model of MHD nanofluid flow having gyrotactic microorganisms with thermal radiation and chemical reaction effects. Khan et al [33] studied magnetic and Navier slip effect in heat and mass transfer in gyrotactic micro-organism in vertical surface. Similarly, Khan with Makinde [34] have been studied boundary layer flow of magnetohydrodynamic (MHD) in Nano-fluid consisting gyrotactic organism in linearly stretching sheet.

In the present field of science and engineering, most of the mathematical problems are so involved that the accurate solution is almost very difficult. So for the solution of such problems, Analytical and Numerical methods are used to find the approximate solution. One of the most famous methods for solving such type problems is Homotopy Analysis Method (HAM). Its main advantage is applying to the nonlinear differential equations without discretisation and linearization. In (1992) Liao [35-37] was the first one to examine this method for the solution of non-linear comlicated problem's and showed that this method is quickly convergent to the approximate solution. The solution by this technique is perfect because it contains all the embeded parameters of a problem and we can easily explain its behaviour in detail. Due to its quick convergence, many researchers like Abbasbandy [38] and Rashidi [39] have used this technique to solve highly nonlinear and coupled equations. The basic theme of this paper is to discuss the unsteady bioconvection thermally conducting squeezing flows of a nanofluid between parallel plates in the occurrence of Gyrotactic Micro-organisms. To our knowledge, no studies have been made to analyze the simultaneous effects of heat generation/absorption on heat and mass transfer of Squeezing nanofluid between two parallel channels. The governing coupled nonlinear partial differential equations are reduced to a system of coupled ordinary differential equations using appropriate transformations, and then the resulting equations are solved analytically by the homotopy analysis method (HAM). A parametric study is conducted to investigate the influence of various physical parameters on the velocity, temperature, concentration and density of motile microorganism profile.

2 Formulation

The considered flow is thermally conducting incompressible viscous nanofluid with effects of thermal radiations, between two parallel and horizontal plates. The distance between upper and lower plates is represented by h. The Coordinate system is selected in such a method that lower plate is on the horizontal axis (*x*-axis) and the *y*-axis is perpendicular to the lower plate which is assumed to be fixed. The flow of the nanofluid and heat-transfer is assumed in the unsteady two-dimensional states which are laminar, incompressible and stable. Moreover, the upper plate is capable of moving away with velocity $v(t) = \frac{dh}{dt}$.

Uniform temperatures given to the lower plate is T_1 and at upper plate is represented by T_2. Where upper plate has reflexive supporting conditions, and nano-particles are scattered uniformly at the lower plate shown in Fig. 1. Uniform microorganisms distribution on the lower plate represented by N_1 and upper plate denote by N_2. The geometry of the nanofluid flow model is shown in the Fig. 1.

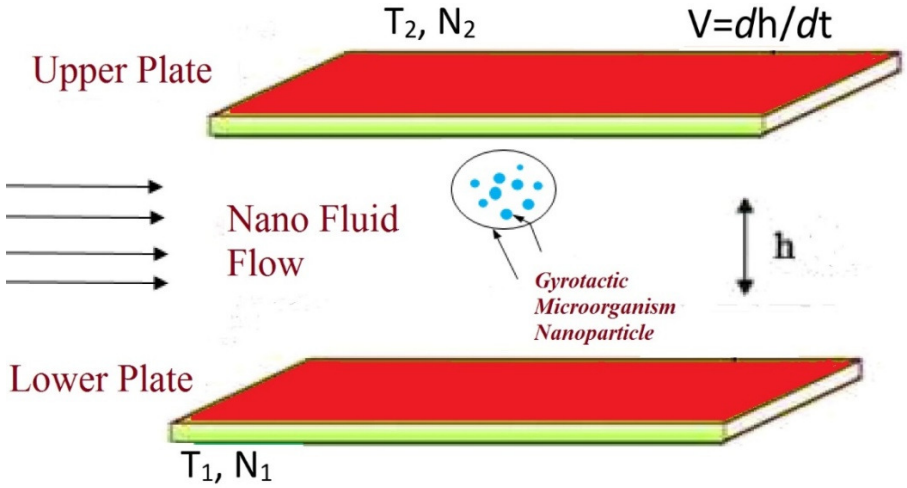

Fig. 1. Sketch of the Nanofluid flow model

The governing equations of Continuity, Velocity, Temperature, Concentration and Density of the motile microorganism are articulated as follow,

$$u_x + v_y = 0, \tag{1}$$

$$\rho_{nf}\left(u_t + uu_x + vv_y\right) = -p_x + \mu\left(u_{xx} + v_{yy}\right) \tag{2}$$

$$\rho_{nf}\left(v_t + uv_x + vv_y\right) = -p_y + \mu\left(v_{xx} + v_{yy}\right), \tag{3}$$

$$\left(T_t + uT_x + vT_y\right) = \hat{\alpha}\left(T_{xx} + T_{yy}\right) + \tau\left[D_B\left\{C_xT_x + C_yT_y\right\} + \left(\frac{D_T}{T_0}\right)\left\{\left(T_x\right)^2 + \left(T_y\right)^2\right\}\right] - \frac{1}{\left(\rho c_p\right)_f}\left(q_{rd}\right)_y, \tag{4}$$

$$C_t + uC_x + vC_y = D_B\left[C_{xx} + C_{yy}\right] + \frac{D_T}{T_0}\left[T_{xx} + T_{yy}\right], \tag{5}$$

$$N_t + uN_x + vN_y + \left(\mathrm{N}v^*\right)_z = D_nN_{yy}. \tag{6}$$

The equations. (1-6) represents the flow model for nanofluid. In above mentioned equations u and v denotes velocity components, N be the density of the motile-microorganism, T and C shows the temperature at the plate and volumetric fraction of the nanoparticles, $\tau = \dfrac{\left(\rho c\right)_p}{\left(\rho c\right)_f}$, where $(\rho c)_p$ & $(\rho c)_f$

represents temperature capacity of nanoparticles and fluids. Moreover, μ denotes viscosity, D_B represents Brownian diffusion and D_T denotes thermophoretic coefficient, in x and y direction respectively. Further $v^* = \frac{(bw_c)}{\Delta C} C_y$. In Eq (4), q_{rd} is the radiative heat fluctuation is expressed in term of Roseland approximation as:

$$q_{rd} = -\frac{16\sigma^*}{3\mathrm{K}^*} T_y, \tag{7}$$

In equation (7) relation σ^* represents "Stefan Boltzmann" constant and k^* indicate "mean absorption" coefficient respectively. Supposing that the difference in heat inside the flow is such that T^4 can be expressed as a linear combinations of the heat, we enlarge T^4 as Taylor's series about T_0 as under:

$$\mathrm{T}^4 = \mathrm{T}_0^4 + 4\mathrm{T}_0^3 \left(\mathrm{T} - \mathrm{T}_0\right) + ..., \tag{8}$$

After neglecting terms of higher order we obtained:

$$\mathrm{T}^4 \cong -3\mathrm{T}_0^4 + 4\mathrm{T}_0^3 \mathrm{T}, \tag{9}$$

By Putting Eq. (8) in Eq. (7) we get

$$\left(q_{rd}\right)_y = -\frac{16\mathrm{T}_0^3 \sigma^*}{3K^*} T_{yy}, \tag{10}$$

Feasible auxiliary conditions for lower and upper plates are:

$$v = 0,\ u = 0,\ \ C = C_0,\ \mathrm{T} = \mathrm{T}_1 \text{ and } N = \mathrm{N}_1, \tag{11}$$

$$v = \frac{dh}{dt},\ u = 0,\ \ \mathrm{T} = T_2,\ D_B\left(\frac{\partial C}{\partial y}\right) + \frac{D_T}{\mathrm{T}_0}\left(\frac{\partial \mathrm{T}}{\partial y}\right) = 0 \text{ and } N = \mathrm{N}_2. \tag{12}$$

Similarity Variables are:

$$\Psi(x, y) = \left(\frac{1-\alpha t}{bv}\right)^{\frac{-1}{2}} xf(\eta), u = \left(\frac{1-\alpha t}{bx}\right)^{-1} f'(\eta), v = -\left(\frac{1-\alpha t}{bv}\right)^{\frac{-1}{2}} f(\eta), \eta = \left(\frac{v(1-\alpha t)}{b}\right)^{\frac{-1}{2}} y,$$
$$\theta(\eta) = \left(\frac{\mathrm{T} - \mathrm{T}_0}{\mathrm{T}_2 - \mathrm{T}_0}\right), \phi(\eta) = -1 + \frac{C}{C_0} \text{ and } \varphi(\eta) = \left(\frac{\mathrm{N} - \mathrm{N}_0}{\mathrm{N}_2 - \mathrm{N}_0}\right). \tag{13}$$

In above expression $\mathrm{T}_0, C_0,$ and N_0 are reference temperature, reference concentration of nanoparticles and reference concentration of microorganism respectively.

Substituting Eq. (13) into the governing Eqs. (1) to (6), clearly equation (1) hold identically and Eqs. (2-5) gives us the following ordinary differential equations.

$$f^{iv} + ff''' - f'f'' - \lambda\eta f''' - 3\lambda f'' = 0, \tag{14}$$

$$\left(1+\frac{4}{3}\mathrm{Rd}\right)\theta'' + \mathrm{Pr}\left(f - \lambda\eta\right)\theta' + Nb\phi'\theta' + Nt\left(\theta'\right)^2 = 0, \tag{15}$$

$$\phi'' + Le\left(f - \lambda\eta\right)\phi' + \left(\frac{\mathrm{N}t}{\mathrm{N}b}\right)\theta'' = 0, \tag{16}$$

$$\varphi'' + Sc(f - \lambda\eta)\varphi' - Pe\varphi\phi'' - Pe\varphi'\phi' = 0. \tag{17}$$

The non-dimensional parameters are:

$$\begin{aligned}
&\lambda = \frac{\alpha}{2b},\ \ Rd = \frac{4T_0^{\,3}\sigma^*}{3\left(\rho c_p\right)_f k\alpha}, Nb = \frac{(\rho c)_p}{(\rho c)_f}\frac{D_b C_0}{\alpha}, \mathrm{Pr} = \frac{v}{\alpha}, Le = \frac{v}{D_B},\\
&\mathrm{N}t = \frac{(\rho c)_p}{(\rho c)_f}\frac{D_T(\mathrm{T}_2 - \mathrm{T}_0)}{\mathrm{T}_0\alpha}, \qquad Sc = \frac{v}{D_n},\ \ Nb = \frac{(\rho c)_p}{(\rho c)_f}\frac{D_b C_0}{\alpha},\\
&Pe = \frac{b_c W_c}{D_n},\ \ \omega = \frac{\alpha H}{2(vb)^{\frac{1}{2}}}, \delta\theta = \frac{(\mathrm{T}_1 - \mathrm{T}_0)}{(\mathrm{T}_2 - \mathrm{T}_0)}.\ \delta\varphi = \frac{(\mathrm{N}_1 - \mathrm{N}_0)}{(\mathrm{N}_2 - \mathrm{N}_0)},\ \ \delta\phi = \left(\frac{C_1 - C_0}{C_0}\right),
\end{aligned} \tag{18}$$

In equations (14-17) different parameters are used like λ represent unsteady squeezing parameter, The other dimensionless physical parameter which are used in the Flow Model are radiation (Rd) , Brownian motion $\left(Nb\right)$, Peclet (Pe), , thermophoresis parameter (Nt), Levis number $\left(\mathrm{Le}\right)$, Prandtl number (Pr) and Schmidt number $\left(Sc\right)$. Also ω, δ_ϕ, δ_φ and δ_θ all are constants. Furthermore, transmuted form of the feasible boundary conditions both for lower as well as for upper plates defined in equations (11) to (12) are as:

$$\begin{aligned}
&f(0) = 0, f'(0) = 0, f'(1) = 0, \theta(1) = \delta_\theta, f(1) = w,\\
&\theta(0) = 1, \varphi(1) = \delta_\varphi, \phi(1) = \delta_\phi\ , \varphi(0) = 1,\\
&\phi(0)\mathrm{N}b + \theta'(0)\mathrm{N}t = 0.
\end{aligned} \tag{19}$$

The "skin-friction", "Nusselt-Number", "Sherwood-Number" and the "Density-Number of the motile microorganism" are defined under as:

$$\begin{aligned}
&C_f = \frac{2\tau\omega}{\rho U_\omega^{\,2}}, \mathrm{Nu}_x = \frac{x\,\mathrm{q}_w}{\mathrm{K}\left(\mathrm{T}_w - \mathrm{T}_0\right)}, Sh_x = \frac{xq_m}{D_B\left(C_w - C_0\right)}, \mathrm{N}n_x = \frac{xq_n}{D_n\left(n_w - n_0\right)},\\
&\tau_\omega = \left|\mu\frac{\partial u}{\partial y}\right|_{y=0}, q_\omega = \left|\mathrm{K}\frac{\partial \mathrm{T}}{\partial y}\right|_{y=0}, q_m = \left|-D_B\frac{\partial\phi}{\partial y}\right|_{y=0}\ \ \&\ q_n = \left|-D_n\frac{\partial\zeta}{\partial y}\right|_{y=0}.
\end{aligned} \tag{20}$$

In above expression $T_w, C_w,$ and n_w are surface temperature, surface concentration of nanoparticles and surface concentration of microorganism respectively.

By applying Eq. (13) dimensionless form, Nusselt Number, skin-Friction, Sherwood Number and Local-Density of motile microorganism are as:

$$\frac{\sqrt{\mathrm{Re}_x}}{2} C_f = f''(0), Nu_x \,\mathrm{Re}_x^{\frac{-1}{2}} = -\theta'(0), Sh_x \,\mathrm{Re}_x^{\frac{-1}{2}} = -\phi'(0) \;\; \& \;\; Nn_x \,\mathrm{Re}_x^{\frac{-1}{2}} = -\xi'(0) \tag{21}$$

Where $\mathrm{Re}_x = \frac{xU_\omega}{v}$ is a local Reynolds number and U_w is the stretching velocity.

3 Methodology

The above mentioned coupled differential equation (14) - (17) with boundary conditions defined in equation (19), are tackled trough analytical technique called Homotopy Analysis Method" (HAM). Since the present mathematical model contains boundary value problem (BVP) so these equations are solved with the help of Homotopy Analysis Method" (HAM).All these working schemes are assimilated in the computational software Mathematica.

4 Solution by HAM

In order to solve Eqs. [14-17] along with boundary conditions (19), we using "HAM". For the solution HAM scheme has benefits such as it is free from the large or small parameters. This technique gives a simple way to confirm the convergence of the solution. . Moreover, it delivers freedom for the right selection of auxiliary parameter & base function. In this scheme, the assisting parameters $\hbar$ are used to control the convergence of the problem. Initial guesses are carefully chosen as:

$$\begin{aligned} &f_o(\eta)=3\omega\eta^2-2\omega\eta^3,\ \theta_0(\eta)=1-\eta+\delta_\theta\eta, \\ &f_o(\eta)=\frac{1}{Nb}(-Nt+Nt\eta+Nt\delta_\theta-Nt\delta_\theta\eta+Nb\delta_f), \\ &\varphi_o(\eta)=1-\eta+\delta_\varphi\eta \end{aligned} \tag{22}$$

Selected linear operators, are:

$$L_f(f)=\frac{\partial^4 f}{\partial\eta^4},\ L_\theta(\theta)=\frac{\partial^2\theta}{\partial\eta^2},\ L_\phi(\phi)=\frac{\partial^2\phi}{\partial\eta^2},\ L_\varphi(\varphi)=\frac{\partial^2\varphi}{\partial\eta^2}. \tag{23}$$

The above-mentioned differential operator's contents are shown below:

$$L_f(\varepsilon_1+\varepsilon_2\eta+\varepsilon_3\eta^2+\varepsilon_4\eta^3)=0, \boldsymbol{L}_\theta(\varepsilon_5+\varepsilon_6\eta)=0, \boldsymbol{L}_\phi(\varepsilon_7+\varepsilon_8\eta)=0, \boldsymbol{L}_\varphi(\varepsilon_9+\varepsilon_{10}\eta)=0. \tag{24}$$

Here $\sum_{i=1}^{10}\varepsilon_i$ where $i=1,2,3...$ denotes arbitrary constants.

The resultant non-linear operators are given by: N_f, N_θ, N_φ, and N_ϕ

$$\mathrm{N_f}\left(\mathrm{f}(\eta;\psi)\right)=\frac{\partial^4 \mathrm{f}(\eta;\psi)}{\partial\eta^4}+\mathrm{f}(\eta;\psi)\frac{\partial^2 \mathrm{f}(\eta;\psi)}{\partial\eta^2}-\frac{\partial \mathrm{f}(\eta;\psi)}{\partial\eta}\times\frac{\partial^2 \mathrm{f}(\eta;\psi)}{\partial\eta^2}-\lambda\eta\frac{\partial^3 \mathrm{f}(\eta;\psi)}{\partial\eta^3}$$
$$-3\lambda\frac{\partial^2 \mathrm{f}(\eta;\psi)}{\partial\eta^2}, \tag{25}$$

$$\mathrm{N_\theta}\left(\theta(\eta;\psi),\mathrm{f}(\eta;\psi),\phi(\eta;\psi)\right)=\left(1+\frac{4}{3}\mathrm{Rd}\right)\frac{\partial^2\theta(\eta;\psi)}{\partial\eta^2}+\mathrm{Pr}\left(\mathrm{f}(\eta;\psi)\text{-}\lambda\eta\right)\frac{\partial\theta(\eta;\psi)}{\partial\eta}$$
$$+\mathrm{Nb}\frac{\partial\theta(\eta;\psi)}{\partial\eta}\frac{\partial\phi(\eta;\psi)}{\partial\eta}+\mathrm{Nt}\left(\frac{\partial\theta(\eta;\psi)}{\partial\eta}\right)^2, \tag{26}$$

$$\mathrm{N_\phi}\left(\phi(\eta;\psi),\mathrm{f}(\eta;\psi),\theta(\eta;\psi)\right)=\frac{\partial^2\phi(\eta;\psi)}{\partial\eta^2}+\mathrm{Le}\left(\mathrm{f}(\eta;\psi)\text{-}\lambda\eta\right)\frac{\partial\phi(\eta;\psi)}{\partial\eta}$$
$$+\left(\frac{\mathrm{Nt}}{\mathrm{Nb}}\right)\frac{\partial^2\theta(\eta;\psi)}{\partial\eta^2}, \tag{27}$$

$$\mathrm{N_\varphi}\left(\varphi(\eta;\psi),\mathrm{f}(\eta;\psi),\phi(\eta;\psi)\right)=\frac{\partial^2\varphi(\eta;\psi)}{\partial\eta^2}-\mathrm{Pe}\varphi(\eta;\psi)\frac{\partial^2\phi(\eta;\psi)}{\partial\eta^2}-Pe\frac{\partial\phi(\eta;\psi)}{\partial\eta}\frac{\partial\varphi(\eta;\psi)}{\partial\eta}+$$
$$\mathrm{Sc}\left(\mathrm{f}(\eta;\psi)\text{-}\lambda\eta\right)\frac{\partial\varphi(\eta;\psi)}{\partial\eta}. \tag{28}$$

4.1 Zeroth order deformation problem

$$(1\text{-}\psi)\mathrm{L_f}\left(\mathrm{f}(\eta,\psi)\text{-}\mathrm{f_0}(\eta)\right)\text{-}\psi\mathrm{h_f}\mathrm{N_f}\left(\mathrm{f}(\eta,\psi)\right)=0, \tag{29}$$

$$(1\text{-}\psi)\mathrm{L_\theta}\left(\theta(\eta,\psi)\text{-}\theta_0(\eta)\right)\text{-}\psi\mathrm{h_\theta}\mathrm{N_\theta}\left(\theta(\eta;\psi),\mathrm{f}(\eta;\psi),\mathrm{f}(\eta;\psi)\right)=0, \tag{30}$$

$$(1\text{-}\psi)\boldsymbol{L}_\phi\left(\phi(\eta,\psi)-\phi_0(\eta)\right)\text{-}\psi h_\phi\mathrm{N}_\phi\left(\phi(\eta;\psi),\mathrm{f}(\eta;\psi),\theta(\eta;\psi)\right)=0, \tag{31}$$

$$(1\text{-}\psi)\boldsymbol{L}_\varphi\left(\varphi(\eta;\psi)-\varphi_0(\eta)\right)\text{-}\psi\mathrm{h}_\varphi\mathrm{N}_\varphi\left(\varphi(\eta;\psi),\mathrm{f}(\eta;\psi),\phi(\eta;\psi)\right)=0. \tag{32}$$

The subjected boundary conditions are:

$$\mathrm{f}(\eta;\psi)\Big|_{\eta=0}=0,\ \left.\frac{\partial\mathrm{f}(\eta;\psi)}{\partial\eta}\right|_{\eta=0}=0,\ \mathrm{f}(\eta;\psi)\Big|_{\eta=1}=w,\ \left.\frac{\partial\mathrm{f}(\eta;\psi)}{\partial\eta}\right|_{\eta=1}=0,$$
$$\phi(\eta;\psi)\Big|_{\eta=1}=\delta_\phi,\ \varphi(\eta;\psi)\Big|_{\eta=0}=1,\ \varphi(\eta;\psi)\Big|_{\eta=1}=\delta_\varphi,\ \theta(\eta;\psi)\Big|_{\eta=0}=1,$$
$$\theta(\eta;\psi)\Big|_{\eta=1}=\delta_\theta,\ \mathrm{Nb}\phi(\eta;\psi)\Big|_{\eta=0}+\mathrm{Nt}\left.\frac{\partial\theta(\eta;\psi)}{\partial\eta}\right|_{\eta=0}=0. \tag{33}$$

Where $\psi \in [0,1]$ is the imbedding constraint, $\hbar_f$, $\hbar_\theta$, $\hbar_\varphi$ and $\hbar_\phi$ were used to regulate convergence of the solution. Where $\psi = 0$ & $\psi = 1$ we have:

$$f(\eta;1) = f(\eta),\ \theta(\eta;1) = \theta(\eta),\ \phi(\eta;1) = \phi(\eta) \text{ and } \varphi(\eta;1) = \varphi(\eta).$$

Expanding the above term of ψ with the use of Taylor's series expansion we obtain:

$$\begin{aligned} &f(\eta,\psi) = f_o(\eta) + \sum_{i=1}^{\infty} f_i(\eta),\ 0 = \theta_o(\eta) + \sum_{i=1}^{\infty} \theta_i(\eta) - \theta(\eta,\psi), \\ &\phi(\eta,\psi) = \phi_o(\eta) + \sum_{i=1}^{\infty} \phi_i(\eta),\ 0 = \varphi_o(\eta) + \sum_{i=1}^{\infty} \varphi_i(\eta) - \varphi(\eta,\psi). \end{aligned} \tag{34}$$

Where

$$\begin{aligned} &f_i(\eta) = \frac{1}{i!}\frac{\partial f(\eta;\psi)}{\partial \eta}\bigg|_{\psi=0},\ \theta_i(\eta) = \frac{1}{i!}\frac{\partial \theta(\eta;\psi)}{\partial \eta}\bigg|_{\psi=0}, \\ &\phi_i(\eta) = \frac{1}{i!}\frac{\partial \phi(\eta;\psi)}{\partial \eta}\bigg|_{\psi=0},\ \varphi_i(\eta) = \frac{1}{i!}\frac{\partial \varphi(\eta;\psi)}{\partial \eta}\bigg|_{\psi=0}. \end{aligned} \tag{35}$$

4.2 I^{th} order deformation problem

$$\begin{aligned} &L_f\left(f_i(\eta) - \xi_i f_{i-1}(\eta)\right) = h_f R_i^f(\eta),\ L_\theta\left(\theta_{ii}(\eta) - \xi_i \theta_{i-1}(\eta)\right) = h_\theta R_i^\theta(\eta), \\ &L_\varphi\left(\varphi_i(\eta) - \xi_i \varphi_{i-1}(\eta)\right) = h_\varphi \Re_i^\varphi(\eta), L_\phi\left(\phi_i(\eta) - \xi_i \phi_{i-1}(\eta)\right) = h_\phi \Re_i^\phi(\eta). \end{aligned} \tag{36}$$

The resultant boundary conditions are:

$$\begin{aligned} &f_i(0)=0,\ f_i'(0)=0,\ f_i(1)=0,\ f_i'(1)=0,\ \theta_{ii}(0)=0,\ \theta_{ii}(1)=0, \\ &Nbf_i(0)+Nt\theta_i'(0)=0,\ \phi_i(1) = 0,\ \varphi_{ii}(0) = 0,\ \varphi_{ii}(1) = 0. \end{aligned} \tag{37}$$

$$R_i^f(\eta) = f_{i-1}^{iv} + \sum_{k=0}^{i-1} f_{i-1-k} f_k''' - \sum_{k=0}^{i-1} f_{i-1-k}' f_k'' - \lambda\eta f_{i-1}''' - 3\lambda f_{i-1}'', \tag{38}$$

$$R_i^\theta(\eta) = \left(1 + \frac{4}{3}Rd\right)\theta_{i-1}'' + Pr\left(\sum_{k=0}^{i-1} f_{i-1-k}\theta_k' - \lambda\eta\theta_{i-1}'\right) + Nt\sum_{k=0}^{i-1}\theta_{i-1-k}'\theta_k' + Nb\sum_{k=0}^{i-1} f_{i-1-k}'\theta_k', \tag{39}$$

$$\Re_i^\phi(\eta) = \phi_{i-1}'' + \left(\frac{Nt}{Nb}\right)\theta_{i-1}'' + Le\left(\sum_{k=0}^{i-1} f_{i-1-k}\phi_k' - \lambda\eta\phi_{i-1}'\right), \tag{40}$$

$$\Re_i^\varphi(\eta) = \varphi_{i-1}'' - Pe\sum_{k=0}^{i-1}\varphi_{i-1-k}\phi_k'' - Pe\sum_{k=0}^{i-1}\varphi_{i-1-k}'\phi_k' + Sc\left(\sum_{k=0}^{i-1} f_{i-1-k}\varphi_k' - \lambda\eta\ \varphi_{i-1}'\right). \tag{41}$$

Where

$$\xi_i = \begin{cases} 1, & \text{if } \psi > 1 \\ 0, & \text{if } \psi \le 1 \end{cases} \tag{42}$$

5 Convergence

This segment of the article about HAM Convergence solution. When the series solutions are computed for the velocity, density of motile microorganism, temperature and concentration functions via using HAM, the assisting parameters are $\hbar_f$, $\hbar_\varphi$, $\hbar_\theta$, $\hbar_\phi$. These main parameters are responsible for the convergence of the solution. Table 1 displays numerical values of HAM solutions at different approximation using various values of different parameters. It is clear from the Table 1 that homotopy analysis technique is a quickly convergent technique.

Table 1. Shows Convergence of the HAM up to 17th Order Approximation where, $\lambda = Nt = 0.4$, $Rd = 0.2, \Pr = 0.7, Nb = 1, Le = 0.6, Sc = 0.8$ and $Pe = 0.6$.

Approximation Order.	$f''(0)$	$\theta'(0)$	$\phi'(0)$	$\varphi'(0)$
1	3.98886	-0.0207921	0.953750	1.00025
3	3.97650	-0.0387064	0.913169	1.07375
5	3.97584	-0.0396453	0.910490	1.08915
7	3.97583	-0.0396677	0.910383	1.09009
9	3.97583	-0.0396681	0.910378	1.09013
13	3.97583	-0.0396682	0.910379	1.09014
15	3.97583	-0.0396682	0.910379	1.09014
17	3.97583	-0.0396682	0.910379	1.09014

6 Results and Discussion

The current research has been carried out to study the Bioconvection model for squeezing flow between parallel plates containing gyrotactic microorganisms under the influence of thermal radiation and heat generation/absorption. The determination of this subsection is to examine the physical outcomes of dissimilar embedding on the Velocity $f(\eta)$, Heat $\theta(\eta)$, Concentration $\phi(\eta)$ and Density of motile microorganism $\varphi(\eta)$ distribution which are illustrated in (Figs. 2-15). Fig. 1 shows the geometry of the fluid model.

6.1 Influence of squeezing fluid parameter

Figs. 2, 3, 4 & 5 shows the impacts of squeezing fluid parameter λ on $f(\eta)$, $\theta(\eta)$, $\phi(\eta)$ & $\varphi(\eta)$. When plates are moving apart, then λ takes the positive value in that corresponding case & when plates are coming closer the values are considered negative. Fig. 2 shows the influence of the flow when plates are moving away & this is opposite case of when plates are coming nearer. With the increase of λ values fluid velocity also increasing. Clearly velocity increases in the channel when fluid sucked inside. On the other hand when fluid injected out, then the plates come closer to one another. This manner brings about a drop in the fluid and consequently decreases the velocity. With the varying value of λ parameter the influence of

$f(\eta)$ shown in Fig. 2. Figs. 3 and 4 show the influence of λ parameter on the heat and concentration distributions respectively. Due to squeezing of the fluid the velocity increases and subsequently falls the temperature of the fluid because warm nanoparticles are escaping rapidly which results in lower temperature and the concentration of the fluid automatically reduces. Fig. 5 indicates variation in density of the motile microorganism for various values of λ. The density of microorganisms $\varphi(\eta)$ illustrates variations. With changing λ values, the $\varphi(\eta)$ is a decreasing factor, when λ parameter changes negatively and it shows increasing function for positive values of λ.

6.2 Influence of Prandtl number parameter

The impact of $\Pr$ on the $\theta(\eta)$ & $\phi(\eta)$ are presented in Figs. 6 and 7. Clearly it is seen that temperature and concentration distributions vary inversely with $\Pr$, that is temperature distribution drop with large numbers of $\Pr$ and rise for lesser values of $\Pr$. Physically, the fluids having a small number of $\Pr$ has larger thermal diffusivity and this effect is opposite for higher Prandtl number. Due to this fact large $\Pr$ cause the thermal boundary layer to decreases. The effect is even more diverse for the small number of $\Pr$ since thermal boundary layer thickness is relatively large. On the other hand, increasing behaviour of concentration distribution is shown in Fig. 7 for increasing $\Pr$ values.

6.3 Influence of thermophporetic parameter

The Fig. 8 represents the influence of thermophoretic parameter Nt on heat profile $\theta(\eta)$. It is investigated that $\theta(\eta)$ is increased by varying thermophoretic parameter Nt. According to Kinetic Molecular theory increasing the number of particles & increasing number of active particles both can cause to increase in the heat factor. Fig. 9 represents the change in the concentration profile $\phi(\eta)$ due to change in the parameter Nt. The profile $\phi(\eta)$ decreases in suction and injection cases. In injection case, the decrement in $\phi(\eta)$ is slow as compare to fluid suction case.

6.4 Influence of Brownian motion parameter

The Figs. 10 and 11 shows the effect of Nb on $\theta(\eta)$ & $\phi(\eta)$ fields. Heat profile $\theta(\eta)$ is increased by varying values of Nb as shown in Fig. 10. Due to Kinetic molecular theory, the heat of the fluid increases due to the increase of Brownian motion. So the given result is in good agreement with the real situation. Similarly, Fig. 11 highlights the impact of the varying Nb parameter with respect to the concentration profile $\phi(\eta)$ on the domain, $0 \le \eta \le 1$. An increasing impact of $\phi(\eta)$ observed for both suction and injection in Fig. 11. A fast increment observed in $\phi(\eta)$ for fluid suction as compared to fluid injection.

6.5 Influence of Peclet number parameter

Fig. 12 represents the influence of Peclet number Pe on $\varphi(\eta)$. The values of density field of motile-microorganism increases with increasing value of Pe. Fig. 13 shows the impacts of Sc on density field of motile microorganism $\varphi(\eta)$. The values of density field of the motile microorganisms decrease with increase in the values of Sc. Actually, Schmidt number is the ratio of kinematic viscosity to the mass flux. So when kinematic viscosity increases, then spontaneously the Sc increases and $\varphi(\eta)$ decreases.

6.6 Influence of Lewis number parameter

The Fig. 14 shows the impact of Le on the concentration profile $\phi(\eta)$ where it is decreased when the number Le increases. Actually, it is the ratio of thermal diffusivity to the mass diffusivity. So, when the thermal diffusivity decreases it automatically decreases Le and also decreases concentration field.

6.7 Influence of radiation parameter

The Fig. 15 shows the influence of radiation parameter Rd on the heat profile $\theta(\eta)$. It is observed that temperature profile $\theta(\eta)$ decreases with increasing values of Rd. It is a common observation that radiating a fluid or some other thing can cause to reduce the temperature of that particular.

6.8 Numerical tables and discussions

This segment of the article is dedicated to table discussions. Table 1 shows numerical values of HAM solutions at altered approximation using various values of dissimilar parameters. It is clear from the Table 1 that homotopy analysis technique is a rapidly convergent technique. Physical quantities, such as skin-friction coefficient, heat flux, mass flux and Local-density number of motile microorganisms for engineering importance are calculated in the (Tables 2-5). Table 2 shows the influence of inserting parameters $\lambda, \Pr \& Rd$ on Skin friction C_f. It is seen that rising value of λ increases the skin friction, while the large values of $\Pr, Rd$ reduce C_f. Table 3 scrutinises the impacts of embedding parameters $Nt, Nb, \Pr$ and Rd on heat flux $\mathrm{N}u$. It is seen that increasing values of Nt, Nb and $\Pr$ reduce the heat flux $\mathrm{N}u$, where Rd increase the heat flux when it increased. Table 4 inspects the influences of Nb, Nt and $\mathrm{R}\,d$ on mass flux Sh. The increasing values of $\mathrm{N}b$ reduce the mass flux where $\mathrm{N}t$ increases the mass flux. The higher value of Rd reduce the mass flux. The influences of $Nb, Rd, Nt, Pr \& Le$ on $\varphi'(0)$ are shown in Table 5. The increasing values of Rd, $\Pr$ & Nb increase $\varphi'(0)$, while the greater value of Le & $\mathrm{N}t$ reduce $\varphi'(0)$.

GRAPHS:

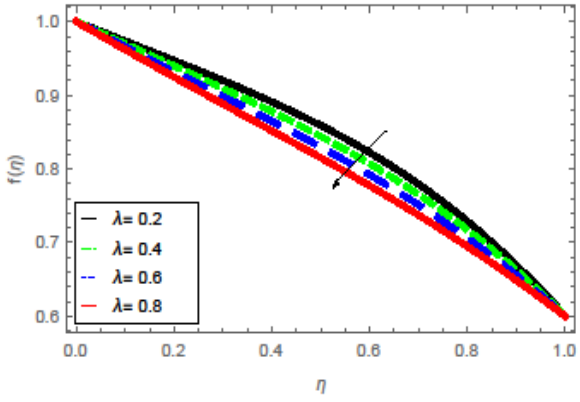

Fig. 2. Effect of λ on $f(\eta)$ when $\omega = 0.9$

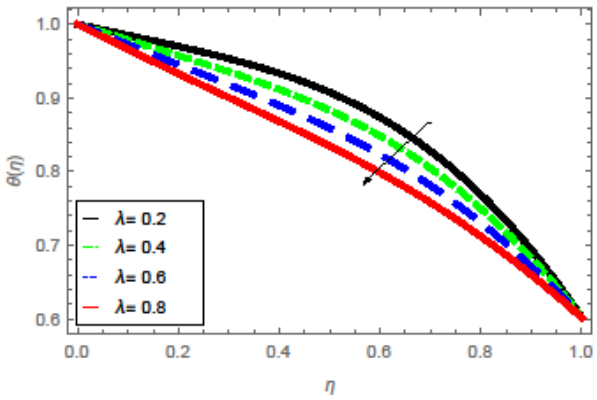

Fig. 3. Effect of λ on $\theta(\eta)$ when

$\omega = 0.9$, $Le = 0.4$, $Nb = 0.3$, $Nt = 0.1$, $\Pr = 0.6$, $Rd = 0.4$.

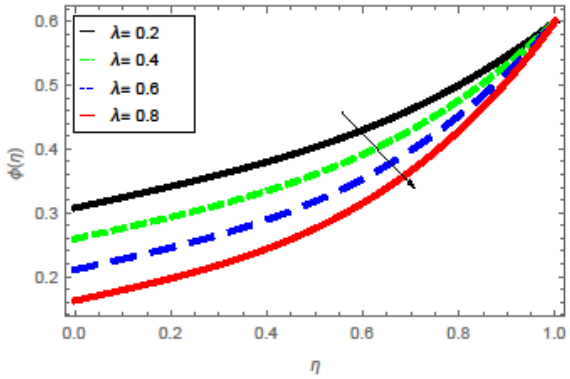

Fig. 4. Effect of λ on $\phi(\eta)$ when

$\omega = 0.9$, $Le = 0.4$, $Nb = 0.3$, $Nt = 0.1$, $\Pr = 0.6$, $Rd = 0.4$.

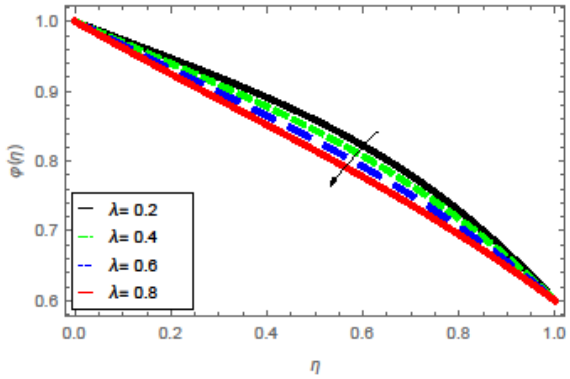

Fig. 5. Effect of λ on $\varphi(\eta)$ when

$\omega = 0.8$, $Le = 0.4$, $Nb = 0.3$, $Nt = Pe = 0.1$

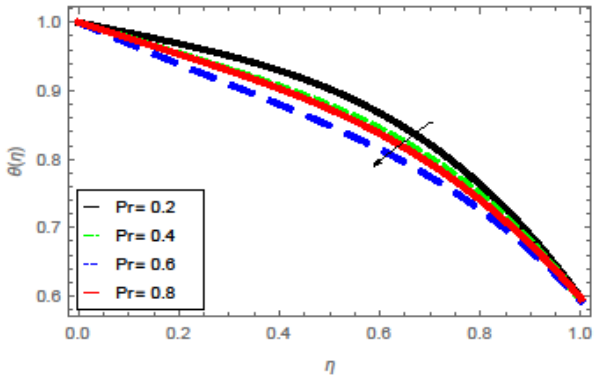

Fig. 6. Effect of Pr on $\theta(\eta)$ when

$\omega = 0.9, Le = 0.3, Nb = 0.1, Nt = 0.6, \lambda = Rd = 0.4$

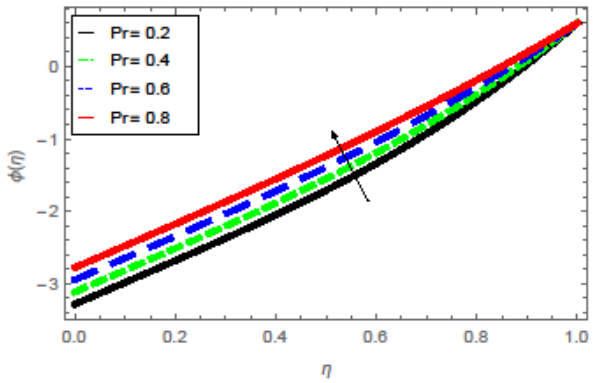

Fig. 7. Effect of Pr on $\phi(\eta)$ when

$\omega = 0.9, Le = 0.3, Nb = 0.1, Nt = 0.6, \lambda = 0.4, \Pr = 0.2$

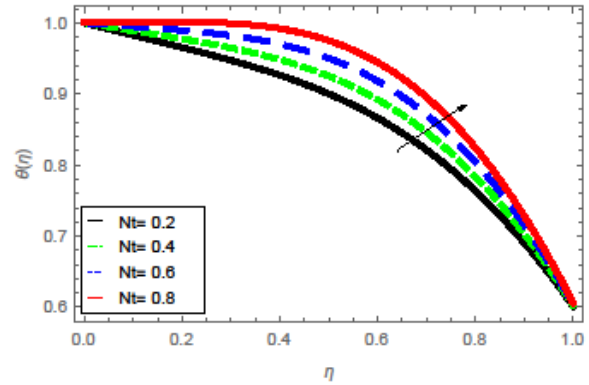

Fig. 8. Effect of Nt on $\theta(\eta)$ when

$\omega = 0.9, Le = 0.3, Nb = 2, \lambda = Rd = 0.4, \Pr = 0.6$

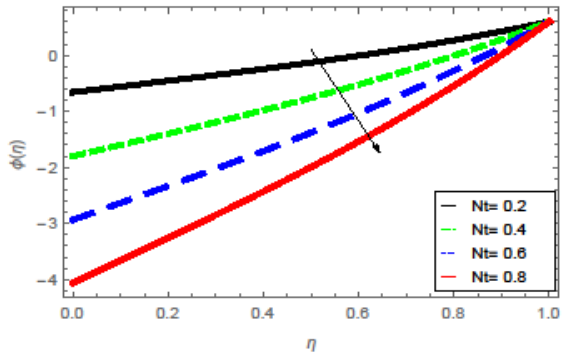

Fig. 9. Effect of Nt on $\phi(\eta)$ when
$\omega = 0.8$, $Le = 0.3$, $Nb = 0.1$, $\lambda = 0.4$, Pr = 0.6

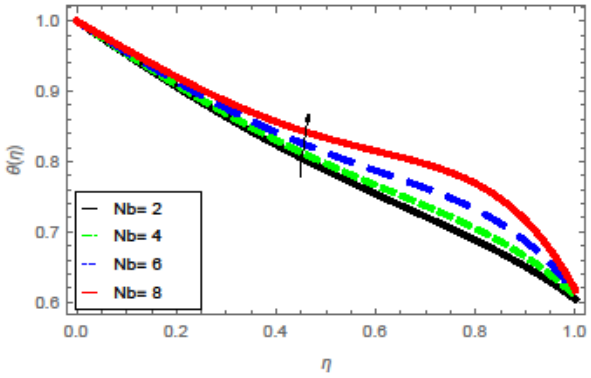

Fig. 10. Effect of Nb on $\theta(\eta)$ when
$\omega = 0.8$, $Le = 0.3$, $Nt = 0.1$, $\lambda = Rd = 0.4$, Pr = 0.6

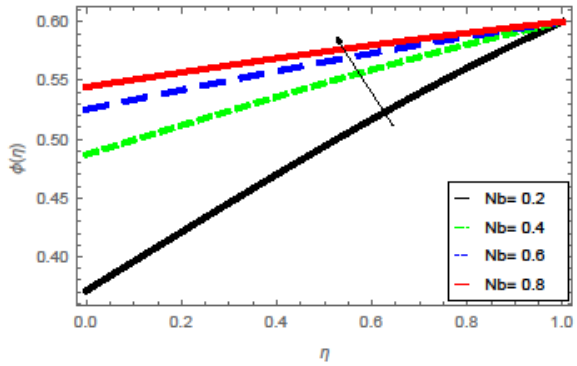

Fig. 11. Effect of Nb on $\phi(\eta)$ when
$\omega = 0.8$, $Le = 0.3$, $Nt = 0.1$, $\lambda = 0.4$, Pr = 0.6

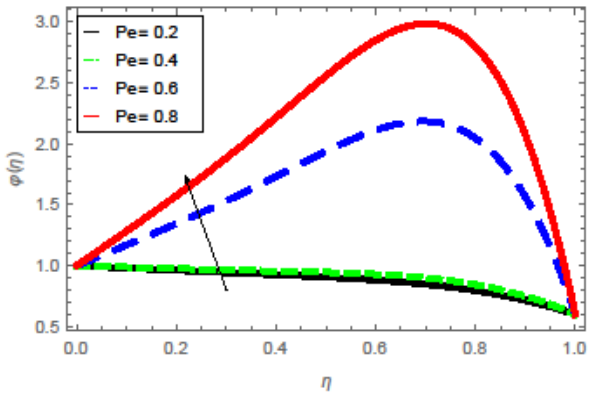

Fig. 12. Effect of Pe on $\varphi(\eta)$ when
$\omega = 0.9, Le = 0.3, Nt = 0.6, Nb = 0.1, \lambda = 0.4$

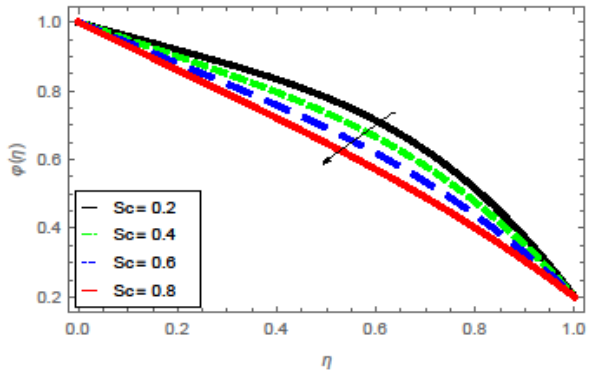

Fig. 13. Effect of Sc on $\varphi(\eta)$ when
$\omega = 0.9, Le = 0.3, Nt = 0.6, Nb = 0.1, \lambda = 0.4, Pe = 0.5$

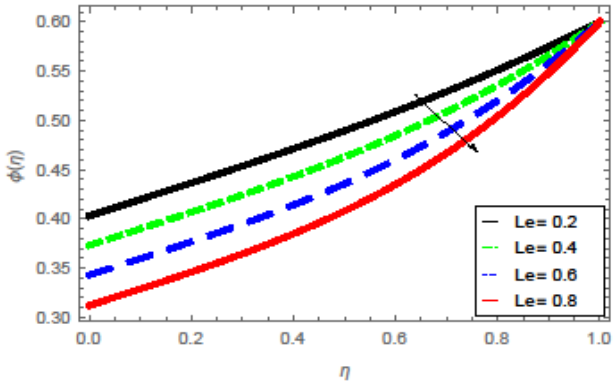

Fig. 14. Effect of Le on $\phi(\eta)$ when
$\omega = 0.9, Le = 0.4, Nt = 0.1, Nb = 0.3, \lambda = 0.4, \mathrm{Pr} = 0.6$

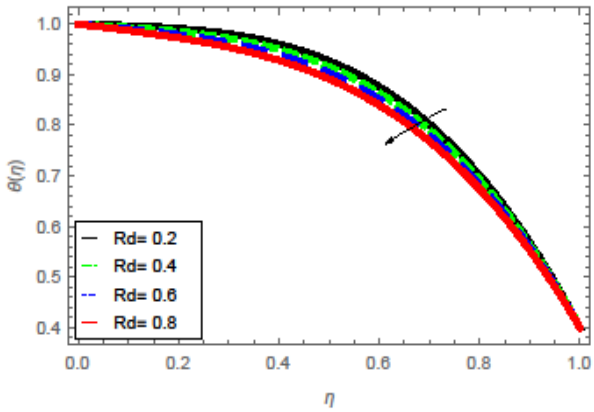

Fig. 15. Effect of Le on $\theta(\eta)$ when
$\omega = Le = 1, \Pr = Nt = 0.6, Nb = 0.1, \lambda = 4$

Table 2. Showing the numerical values of the Skin Friction Co-efficient for various parameters where $Sc = 0.7,\ Pe = 0.6, Nb = 1,\ Nt = Le = 0.5.$

λ	Pr	Rd	$-\left(C_f \operatorname{Re}_x\right)^{\frac{1}{2}}$ **Present results**
1.5			0.9957
2.0			1.2057
2.5			1.4947
	1.0		1.3142
	1.5		1.1245
	2.0		1.0032
		0.5	2.9809
		1.0	2.0011
		1.5	1.3421
		2.0	0.8765

Table 3. Shows the numerical values of Local Nusselt number for unlike type parameters, where $\lambda = 0.5, \Pr = 0.7,\ Le = 0.6,\ Sc = 0.7,\ Pe = 0.6,\ \omega = 0.1,$ and $M = 0.4.$

Nb	Nt	Pr	Rd	$-\theta'(0)$ **Present result**
0.5	0.5	1.0	0.5	1.6450
1.0				1.0174
1.5				1.9501
2.0				1.5546
				1.2013
				1.0569
	0.5			2.5923
	1.0	1.0		1.7456
	1.5	1.5		1.1196
	2.0	2.0		1.0072
	0.5	2.5		2.4609
				2.1796
				1.9406

Nb	*Nt*	Pr	*Rd*	$-\theta'(0)$ **Present result**
			0.5	1.2133
			1.0	1.6202
			1.5	2.0003
			2.0	2.2913

Table 4. Shows the numerical type values of the Local-Sherwood number for unlike parameters Where, λ=M=0.5, Le=0.6, Sc=0.7, Pr=Pe=0.6.

Nb	*Nt*	*Rd*	$-\phi'(0)$ **Present results**
0.2			0.8518
0.6			0.7910
1.0			0.6624
0.2	0.5		0.8615
	1.0		0.9020
	1.5		0.9901
			0.9323
		1.5	1.8555
		2.0	0.9919

Table 5. Shows the Numerical values of Local-density number of motile microorganisms for numerous types of parameters when $\Pr = 1,\ \lambda = M = 0.4,\ Sc = 0.7,$ and $\omega = 0.1,$ **and** $Pe = 0.7.$

Rd	*Nb*	*Nt*	Pr	*Le*	$-\varphi'(0)$ **Present results**
1.0	0.5	0.5	1.0	2.0	0.9542
1.5					1.2526
2.0					1.6434
1.0	0.5				0.9552
	1.0				1.8599
	1.5				2.1053
	0.5	0.5			2.1053
		1.5			1.7801
		2.0			1.6864
		0.5	1.0		2.2592
			5.0		2.3331
			10		2.9533
			1.0	2.0	0.6321
				6.0	0.6254
				10	0.6203

7 Closing Remarks

In the present analysis we have disclosed the characteristics of Bioconvection Model for Squeezing Flow between Parallel Plates Containing Gyrotactic Microorganisms with Impact of Thermal Radiation and Heat Generation/Absorption. The key points are summarized as follows:

- The larger values of *Nb* rises the kinetic energy of the nanoparticles, which result an increase in the heat profile.

- Thermophoretic and Brownian motion parameters affect the concentration field reversely for both the suction and injection case.
- When we increase thermal radiation parameter Rd, then it augments temperature of the boundary layer area in fluid layer. This increase leads to drop in the rate of cooling for nanofluid flow.
- It is observed that $\theta(\eta)$ is increased by varying thermophoretic parameter Nt.
- The convergence of the homotopy method along with the variation of different physical parameters has been observed numerically.
- It is seen that increasing M and λ increase the skin friction, while the large values of Pr *and* Rd reduce C_f.
- The increasing values of $\mathrm{N}b$ reduce the mass flux where $\mathrm{N}t$ increases the mass flux. The higher values of Rd reduce the mass flux.

Competing Interests

Authors have declared that no competing interests exist.

References

[1] Stefan MJ. Versuch Uber die scheinbare adhesion, Sitzungsberichte der Akademie der Wissenschaften in Wien. Mathematik-Naturwissen. 1874;69:713–721.

[2] Verma RL. A numerical solution to squeezing flow between parallel channels. Wear. 1981; 72: 89-95.

[3] Haq RU, Nadeem S, Khan ZH, Noor NFM. MHD squeezed flow of water functionalized metallic nanoparticles over a sensor surface. Physica E: Low-dimensional Systems and Nanostructure. 2015;73:45–53.

[4] Gupta AK, Saha Ray S. Numerical treatment for investigation of squeezing unsteady Nanofluid flow between two parallel plates. Powder Tech. 2015;279:282–289.

[5] Qayyum A, Awais M, Alsaedi A, Hayat T. Unsteady squeezing flow of jeffrey fluid between two parallel disks. Chin. Phys. Lett. 2012;29:034701.

[6] Hayat T, Qayyum A, Alsaedi A. Three-dimensional mixed convection squeezing flow. Appl. Math. Mech. 2015; 36: 47–60.

[7] Hayat T, Abbas T, Ayub M, Muhammad T, Alsaedi A. On squeezed flow of jeffrey nanofluid between two parallel disks. Appl. Sci. 2016;6:346.

[8] Dib A, Haiahem A, Bou-Said B. Approximate analytical solution of squeezing unsteady nanofluid flow. Powder Tech. 2015;269:193–199.

[9] Masuda H, Ebata A, Teramae K, Hishinuma N. Alteration of thermal conductivity and viscosity of liquid by dispersing ultra-fine particles. Netsu Bussei. 1993;7(4):227-233.

[10] Choi SUS. Nanofluids from vision to reality through research. Journal of Heat Transfer. 2009;131: 1–9.

[11] Yu W, France DM, Robert JL, Choi SUS. Review and comparison of nanofluid thermal conductivity and heat transfer enhancement. Heat Transfer Engineering. 2008;29:432-46.

[12] Muhammad S, Ali G, Shah Z, Islam S, Hussain SA. The Rotating Flow of Magneto Hydrodynamic Carbon Nanotubes over a Stretching Sheet with the Impact of Non-Linear Thermal Radiation and Heat Generation/Absorption. Appl. Sci. 2018;8.
DOI: 10.3390/app8040000.

[13] Hamad MAA. Analytical solution of natural convection flow of a nanofluid over a linearly stretching sheet in the presence of magnetic field. International Communications in Heat and Mass Transfer. 2011;38:487–492.

[14] Wong KV, Leon OD. Applications of Nanofluids: Current and Future. Hindawi Publishing Corporation Advances in Mechanical Engineering. 2015;2.
DOI: 10.1155/2010/519659.

[15] Sheikholeslami M, Ganji DD, Javed MY, Ellahi R. Effect of thermal radiation on magneto Hydrodynamics nanofluid flow and heat transfer by means of two phase model. J. Magn. Magn. Mater. 2015;374:36–43.

[16] Hameed K, Muhammad H, Zahir S, Saeed I, Waris K, Muhammad S. The Combined Magneto Hydrodynamic and Electric Field Effect on an Unsteady Maxwell Nanofluid Flow over a Stretching Surface under the Influence of Variable Heat and Thermal Radiation. Appl. Sci. 2018;8.
DOI: 10.3390/app8020160.

[17] Goodman S. Radiant-heat transfer between non gray parallel plates. Journal of Research of the National Bureau of Standards. 1957;58:2732.

[18] Sheikholeslami M, Ganji DD. Three dimensional heat and mass transfer in a rotating system using nanofluid. Powder Technol. 2014;253:789–796.

[19] Sheikholeslami M, Hatami M, Ganji DD. Nanofluid flow and heat transfer in a rotating system in the presence of a magnetic field. J. Of Molecular Liquids. 2014;190:112-120.

[20] Attia HA, Kotb NA. Cairo, Egypt. MHD flow Between Parallel Plates with Heat transfer. Acta Mechanica. 1996;117:215-220.

[21] Mahmoodi M, Kandelousi Sh. Kerosene−alumina nanofluid flow and heat transfer for cooling application. J. Cent. South Univ. 2016;23:983-990.

[22] Mohyud-Din ST, Zaidi ZA, Khan U. Ahmed, N. On heat and mass transfer analysis of the flow of a nanofluid between rotating parallel plates. Aerospace Science and Technology. 2015;46:514-522.

[23] Rokni HB, Alsaad DM, Valipour P. Electro hydrodynamicnanofluid flow and heat transfer between two plates. J. of Molecular Liquids. 2016;216:583–589.

[24] Hayat T, Qayyum A, Alsaadi F, Awais M, Abdullah M, Dobaie MA. Thermal radiation effects in squeezing flow of a Jeffery fluid. Eur. Phys. J. Plus. 2013;128:85.

[25] Ali F, Khan I, Haq SU. Shafie S. Influence of Thermal Radiation on Unsteady Free Convection MHD Flow of Brinkman Type Fluid in a Porous Medium with Newtonian Heating. Mathematical Problems in Engineering; 2013.
DOI.org/10.1155/2013/632394.

[26] Khan SI, Khan U, Ahmed N, Mohyud-Din ST. Thermal Radiation Effects on Squeezing Flow Casson Fluid between Parallel Disks. Communications in Numerical Analysis. 2016; 2016: 92-107.

[27] Srinivasacharya D, Mallikarjuna B, Bhuvanavijaya R. Soret and Dufour effects on mixed convection along a vertical wavy surface in a porous medium with variable properties. Ain Shams Engineering. June 2015;6:553-564.

[28] Alsaedi A, Khan MI, Farooq M, Gull N, Hayat T. Magnetohydrodynamic (MHD) stratified bioconvective flow of nanofluid due to gyrotactic microorganisms. Advanced Powder Technology. 2017;28:288–298.

[29] Bhatti MM, Zeeshan A, Ellahi R. Simultaneous effects of coagulation and variable magnetic field on peristaltically induced motion of Jeffrey nanofluid containing gyrotactic microorganism. Microvascular Research. 2016;110:32-42.

[30] Shahid A, Zhou Z, Bhatti MM, Tripathi D. Magnetohydrodynamics Nanofluid Flow Containing Gyrotactic Microorganisms Propagating Over a Stretching Surface by Successive Taylor Series Linearization Method. Microgravity Science and Technology. 2018;1-11.

[31] Abbas T, Hayat T, Ayub M, Bhatti MM, Alsaedi A. Electromagnetohydrodynamic nanofluid flow past a porous Riga plate containing gyrotactic microorganism. Neural Computing and Applications. 2018;1-9.

[32] Bhatti MM, Mishra SR, Abbas T, Rashidi MM. A mathematical model of MHD nanofluid flow having gyrotactic microorganisms with thermal radiation and chemical reaction effects. Neural Computing and Applications**.** 2016;1-13.

[33] Khan WA, Makinde OD, Khan ZH. The MHD boundary layer flow of a nanofluid containing gyrotactic micro-organisms past a vertical plate with Navier slip. Int. J. Heat Mass Transf. 2014;74:285–291.

[34] Khan WA, Makinde OD. MHD nano fluid bioconvection due to gyrotactic micro-organisms over a convective heat stretching sheet. International Journal of Thermal Sciences. 2014;81: 118-124.

[35] Liao SJ. On the Analytic Solution of Magnetohydrodynamic Flows of Non-Newtonian Fluids over a Stretching Sheet. J. Fluid Mech. 2003;488:189–212.

[36] Liao SJ. On Homotopy Analysis Method for Nonlinear Problems. Appl. Math .Comput. 2004;147:499–513.

[37] Liao SJ. An Analytic Solution of Unsteady Boundary Layer Flows Caused by Impulsively Stretching Plate. Commun. Nonlinear Sci. Numer. Simul. 2006;11:326–339.

[38] Abbasbandy S. Homotopy analysis method for heat radiation equations. International Communications in Heat and Mass Transfer. 2007;34:380-387.

[39] Rashidi MM, Mohimanian SA. Pour. Analytic approximate solutions for unsteady boundary-layer flow and heat transfer due to a stretching sheet by homotopy analysis. Nonlinear Analysis: Modelling and Control. 2010;15:83–95.

Peer-review history:
The peer review history for this paper can be accessed here (Please copy paste the total link in your browser address bar)
http://www.sciencedomain.org/review-history/24973